Single-shot carrier-envelope-phase-tagged ion-momentum imaging of nonsequential double ionization of argon in intense 4-fs laser fields

Nora G. Johnson, O. Herrwerth, A. Wirth, S. De, I. Ben-Itzhak, M. Lezius, B. Bergues, M. F. Kling, A. Senftleben, C. D. Schröter, R. Moshammer, J. Ullrich, K. J. Betsch, R. R. Jones, A. M. Sayler, T. Rathje, K. Rühle, W. Müller, and G. G. Paulus

Phys. Rev. A **83**, 013412 — Published 28 January 2011

DOI: 10.1103/PhysRevA.83.013412

Single-shot carrier-envelope-phase tagged ion-momentum imaging of non-sequential double ionization of argon in intense 4-fs laser fields

Nora G. Johnson[1, 2], O. Herrwerth[1], A. Wirth[1], S. De[2], I. Ben-Itzhak[2], M. Lezius[1], B. Bergues,[1] M. F. Kling[1,2,*]

[1] *Max-Planck-Institut für Quantenoptik, Garching 85748, Germany*

[2] *J. R. Macdonald Laboratory, Department of Physics, Kansas State University, Manhattan, KS 66506, USA*

A. Senftleben[3], C.D. Schröter[3], R. Moshammer[3], J. Ullrich[3]

[3] *Max-Planck-Institut für Kernphysik, Heidelberg, 69117, Germany*

K. J. Betsch[4], R. R. Jones[4]

[4] *University of Virginia, Charlottesville, VA 22904, USA*

A. M. Sayler[5,6], T. Rathje[5,6], Klaus Rühle[5,6], Walter Müller[5,6], G. G. Paulus[5,6,7,*]

[5] *Institut für Optik und Quantenelektronik, Friedrich-Schiller-Universität, Jena, 07743, Germany*

[6] *Helmholtz Institut Jena, 07743 Jena, Germany*

[7] *Department of Physics, Texas A&M University, College Station, Texas 77843, USA*

[*] *Corresponding authors: matthias.kling@mpq.mpg.de; gerhard.paulus@uni-jena.de*

Single-shot carrier-envelope phase (CEP) tagging has been combined with a reaction microscope (REMI) to investigate CEP dependent processes in atoms. Unprecedented experimental stability and data acquisition longevity are achieved. Using this new approach, we studied the CEP effects for non-sequential double ionization (NSDI) of argon in 4 fs laser fields at 750 nm and an intensity of 1.6×10^{14} W/cm^2. The Ar^{2+} ionization yield shows a pronounced CEP dependence which compares well with recent theoretical predictions employing quantitative rescattering theory [1]. Furthermore, we find strong CEP influences on the Ar^{2+} momentum spectra along the laser polarization axis.

The electric field of a laser pulse, $E(t) = E_0(t)\cdot\cos(\omega t + \varphi)$, is fully characterized by the pulse envelope, $E_0(t)$, the carrier frequency, ω, and the carrier-envelope phase (CEP), φ, which is freely adjustable and stabilized in modern laser systems [2]. By manipulating these variables, electron dynamics can be controlled on a sub-femtosecond timescale [3]. A few prominent applications of CEP stable laser pulses are: the reliable and reproducible generation of attosecond light pulses [4], the controlled electron emission from atoms [5-7], and the control of electron localization in the dissociative ionization of molecular hydrogen [8-10] as well as in the more complex multi-electron CO molecule [11]. Most previous experiments employed CEP locking, which results in a signal-to-noise ratio and phase resolution limited by the duration of continuous locking [5, 10]. In addition, a pair of fused silica wedges were used in most previous studies to change the CEP, inherently also modifying the pulse duration and peak intensity by introducing chirp [5, 8, 10, 11]. REMI measurements usually rely on single target particles interacting with individual laser pulses and, therefore, require rather long acquisition times when used with kHz repetition rate laser systems making CEP-dependent REMI studies scarce. The limited duration of continuous CEP locking has triggered studies toward the possibility to measure the CEP as an alternative to CEP-locking [12]. This was recently achieved experimentally for every single laser shot using stereographic detection of electrons from above-threshold ionization (Stereo-ATI) [13] which has also been investigated theoretically [14]Here, we report on the first combination of single-shot phase tagging with a REMI. Our measurements do not require CEP stabilization and allow for long data acquisition times. Furthermore, no dispersive material is required to vary the CEP during the experiment, such that the laser pulse envelope remains constant.

We study the non-sequential double ionization (NSDI) of argon in strong, few-cycle laser fields. NSDI accounts for an enhanced production of doubly charged ions over the yields expected for a purely sequential tunneling mechanism [15]. It is one of the most interesting phenomena in strong-field ionization as it involves the correlated motion of at least two electrons (see e.g. [16]) and many studies have addressed the underlying mechanisms for different target species, pulse durations, intensities, and wavelengths (see e.g. [1, 5, 17-24]). Because of the technical difficulties mentioned above, however, there exists only one measurement with CEP stable few-cycle laser pulses [5]. Such data are highly desirable, as they might further elucidate the sub-cycle electron dynamics responsible for NSDI. Using our new approach, we reinvestigate the NSDI of argon and observe pronounced phase dependences in the double ionization yield and the Ar^{2+} momentum spectra.

The experiments were performed at the AS-1 beamline at the Max Planck Institute of Quantum Optics [25] delivering 4-fs pulses at 750 nm with an energy of 400 μJ / pulse at a 3 kHz repetition rate. The experimental setup is sketched in Fig. 1. Approximately 30 μJ of the beam are focused into a single-shot Stereo-ATI phase meter [13], while the main beam is directed into a vacuum chamber hosting the REMI. The latter is comprised of time-of-flight spectrometers for electrons and ions combined with position sensitive detectors to enable measuring the particles' three-dimensional momentum vectors [26]. The intensity in both devices can be varied by apertures and residual chirp is compensated by fused silica wedges (see Fig. 1). In the REMI chamber, the laser is focused by a spherical mirror (f = 25 cm) into a cold supersonic gas jet of neutral argon atoms. The jet crosses the laser beam slightly before the focus in order to minimize averaging over the CEP due to the Gouy phase shift [27].

The CEP for every single laser shot was determined via a Stereo-ATI measurement [13]. This apparatus utilizes the fact that the shape of the ATI spectrum for ultrashort pulses in Xe, especially for rescattered electrons with high energy, and correspondingly short time-of-flights (TOF), is sensitive to changes in the CEP of the laser pulse [6]. Here, the laser is focused into a xenon target and electrons that are emitted within an angle of approximately 2° around the laser polarization are detected as time-dependent electron currents on the micro-channel plate (MCP) detectors with metal anodes to the left, L, and right, R as depicted in Fig. 1. Converting the two currents into voltages yields the time-dependent ATI spectra in the form of two quickly varying voltage signals.

Fig. 2a and Fig. 2b show TOF spectra for two laser shots with different CEPs. In order to process the ATI spectra and output a signal corresponding to the CEP in real-time, we utilize the fact that there are energy regions in which the contrast or asymmetry, $A = (L\text{-}R) / (L+R)$, in the ATI spectra of Xe varies like sine and cosine of the CEP, $A_1 \approx \sin(\varphi+\varphi_0)$ and $A_2 \approx \cos(\varphi+\varphi_0)$. These energy regions are chosen by appropriate gates in the TOF spectra as depicted in Figs. 2a and 2b (light and dark grey shaded areas). From the integral of the spectra within the gate windows, two asymmetry values A_1 and A_2 can be determined and a parametric asymmetry plot (PAP) of A_1 vs. A_2 can be generated (see Fig. 2c), in which the polar angle θ corresponds to the CEP: $\theta \approx \varphi+\varphi_0$. A specially designed circuit facilitates the calculation of the asymmetry parameters, A_1 and A_2, in ~20 μs [28], thereby allowing the asymmetry parameters to be recorded together with the REMI data simultaneously enabling the phase-tagging of each recorded event.

Although the dependence of the asymmetry parameters on the CEP is only approximated by sine and cosine functions, the exact relationship between φ and θ can be determined based on

the assumption that the laser produces a uniform and random distribution of CEP values. This constraint means that, given enough laser shots, every equally sized interval in φ must have the same number of counts, i.e. $d\varphi = \frac{\rho(\theta)d\theta}{<\rho>} = \lambda(\theta)\mathrm{d}\theta$, where $\rho(\theta)$ is the density of laser shots as a function of θ, $<\rho>$ is the average density, and $\lambda(\theta) \equiv \rho(\theta)/<\rho>$. Therefore, $\varphi(\theta) = \varphi_0 + \int_0^\theta \lambda(\theta')d\theta'$ [29]. The assumption of a uniform distribution is validated by shifting the CEP via tuning the fused silica wedges just before the Stereo-ATI while observing no change in the PAP. Since the REMI data acquisition is triggered only when an event occurs (and therefore the PAP may be biased by recording only these events), we separately recorded unbiased PAP data for the transformation of θ to φ for approximately 10 minutes at the full repetition rate. The transformation from the raw phase, θ, to the actual CEP value, $\varphi+\varphi_0$, for the PAP data displayed in Fig. 2c is shown in Fig. 2d. As can be seen in Fig. 2d, the necessary correction to $\theta = \varphi+\varphi_0$ is small.

In the current measurements our uncertainty in the single-shot CEP detection is less than 210 mrad, which was determined from the PAP data as outlined in Ref. [29]. Note that this uncertainty is comparable to the RMS phase variation obtained by employing a Stereo-ATI as feedback for phase-locking [30]. However, our technique requires neither feedback nor the precise stabilization necessary for locking. Moreover, removing the need for locking and stabilization allows for the collection of data over much longer periods, which, in turn, facilitates a significantly more precise determination of the CEP dependence. Additionally, unlike common locking schemes [2, 31], we measured the CEP after amplification, hollow-core fiber compression, and transport, such that our phase tagging technique accounts for any CEP fluctuations up to the interaction chamber.

Using the described technique, we explored the CEP dependence of NSDI of argon. The prevailing interpretation of NSDI is based on laser-driven rescattering: at a peak of the laser electric field tunnel-ionization produces an electron, which is then driven by the laser field and may recollide with the singly charged ion. Depending on the kinetic energy of the returning electron and the target species, the collision can result in either the direct emission of two electrons in an (e,2e) process (**r**ecollision **i**nduced **d**irect **i**onization, RIDI) or the excitation of the singly charged ion with subsequent field-ionization by the laser field (**r**ecollision **i**nduced **e**xcitation plus **t**unneling, RIET). The electron as well as the doubly charged ion recoil momentum spectra along the laser polarization axis (parallel momentum) exhibit characteristic signatures of the NSDI process: within a classical description the two emitted electrons in an (e,2e) process can acquire up to $p_{||}^{max} = 4\sqrt{U_p}$ (a.u.) [23] where U_p is the ponderomotive potential, defined as $U_p = I/4\omega^2$ (a.u.) for laser intensity I. This simple expression can be derived under the assumption that the two electrons are liberated with zero initial momentum and that the excess energy of the first recolliding electron is consumed completely in the liberation of the second electron. The release of the second electron at recollision energies sufficiently above the threshold for ionization of the ion typically occurs in RIDI when the first electron returns close to its highest kinetic energy near a zero-crossing of the oscillating electric field (corresponding to a maximum in the vector potential $A(t_i)$ at time t_i given by $A(t_i) = -\int_{t_i}^{\infty} E(t)dt$). In this case both electrons are emitted into the same hemisphere along the polarization direction and the momentum distribution of the doubly charged ion exhibits maxima at non-zero momentum [23]. In RIDI, a strong CEP-dependent asymmetry in the electron and ion momentum spectra is expected [22]. In the RIET mechanism, the returning first electron leads to excitation of the singly charged ion. Double ionization occurs in RIET by tunnel

ionization at one of the subsequent peaks of the electric field (near zero of the vector potential). Depending on the sign of the electric field causing tunneling of the second electron it can leave in either the same or the opposite direction as the first, resulting in an ion momentum spectrum with a maximum at zero [23].

Previous studies have shown that both RIDI and RIET typically contribute to NSDI of argon and their importance was studied as a function of the laser pulse duration, intensity and wavelength [5, 16-18, 22-24]. It was found that RIDI dominates NSDI for longer wavelengths and higher intensities due to the higher ponderomotive potential [17]. Liu *et al*. have employed phase-stabilized 5 fs laser pulses at 760 nm and 3.5×10^{14} W/cm^2 and observed a CEP dependence in the parallel Ar^{2+} momentum spectra [5]. Interestingly, a double hump structure in the momentum spectra was obtained for all phases, which indicated a predominant role of RIDI for their experimental parameters [5]. The results were interpreted in terms of a semi-classical model by Rottke *et al.* [22], the validity of which was confirmed by TDSE calculations by Liao *et al.* [20]. Most recently, Micheau *et al*. adapted quantitative rescattering theory to NSDI [1]. They predicted the Ar^{2+} ion yield to be CEP dependent. To date this quantity has not been measured, most likely due to (i) the lack of long-term stability of experiments employing CEP stabilization and (ii) the fact that changing the CEP in previous experiments led to small changes in pulse duration and intensity, thus prohibiting a measurement of the Ar^{2+} yield as a function of CEP alone.

Employing the phase-tagging approach reported here, we have obtained for the first time the CEP dependence of the Ar^{2+} ion yield for constant pulse duration and intensity (see Fig. 3). The peak intensity in our measurement $1.6(\pm0.4)\times10^{14}$ W/cm^2 is determined from the $2U_p$ cutoff in the longitudinal momentum (along the laser polarization axis) of H_2O^+, which was present as

a small background in the jet in our experiments on argon and, in contrast to Ar^+, did not saturate the detector. The experimental Ar^{2+} ion yield data in Fig. 3 is compared to recently published theoretical results by Micheau *et al.* [1]. They calculated the Ar^{2+} yield for a 5 cycle pulse centered at 800 nm at three intensities of $(1.4, 1.6, 2.0)\times10^{14}$ W/cm^2. The theoretical curve for 1.6×10^{14} W/cm^2 agrees best with the data presented here, consistent with the experimentally determined intensity. The calculations predict minima in the Ar^{2+} yield at approximately $3/4\pi$ and $7/4\pi$, which are independent of intensity in this range [1]. In Fig. 3, we choose $\varphi_0 = 0.43\pi$ in the experimental data such that the dip in the total Ar^{2+} yield occurs at the same phase as in the theoretical curves. Although the yield is clearly CEP dependent, it has $\pm\pi$ inversion symmetry. However, this ambiguity can be eliminated by taking the phase-dependent Ar^{2+} momentum spectra into account, which is shown in Fig. 4.

Fig. 4 shows the longitudinal momentum, $p_{||}$, of the Ar^{2+} ions parallel to the laser polarization axis, integrated over the perpendicular momenta. Considering a pulse with $\varphi = 0$, an electron that tunnels out just after the maximum of the laser electric field and recollides about three quarters of a cycle later (near a zero of the electric field and a maximum in the vector potential) gains maximum electron kinetic energy. In this case, the two electrons emitted in an (e,2e) process have positive momentum. Due to momentum conservation, the recoiling Ar^{2+} ion has negative momentum for $\varphi = 0$. Fig. 4a shows a 2D plot of momentum distributions for the full 2π CEP range. The $\pm\pi$ ambiguity present in the CEP dependence of the Ar^{2+} yield is resolved by choosing $\varphi = 0$ for negative Ar^{2+} momentum.

Momentum spectra at four values of φ (integrated over a range of $\pm0.04\pi$) are extracted from Fig. 4a and shown in Fig. 4b. At $\varphi = 0.1$ and 1.1π, the momentum spectra are clearly asymmetric and peak at non-zero momenta, while the spectra at $\varphi = 0.6\pi$ and 1.6π are nearly

identical and centered around zero. Comparison of the data to the earlier work by Liu *et al.* [5] shows that under the current conditions we observe one, not two, peaks in the longitudinal Ar^{2+} momenta for all CEP values. We attribute this difference to the lower intensity used in the present study. Detailed theoretical modeling may give further insight into the corresponding correlated electron dynamics. This however, is beyond the scope of the current paper.

To explore the degree of control reached in our study, Fig. 4c shows the asymmetry in the Ar^{2+} momentum spectra as defined by the parameter $A(\varphi) = (N_-(\varphi)-N_+(\varphi)) / (N_-(\varphi)+N_+(\varphi))$, where N_- and N_+ represent the number of ions with negative and positive $p_{||}$ momenta, respectively. We observe a very high degree of asymmetry of ±0.5 which interestingly fits near-perfectly (adjusted R^2=0.98) to a sine function, as indicated in Fig. 4c.

In conclusion, we combine single-shot CEP-tagging with the REMI technique to allow studies on phase-dependent processes with high statistics and a correspondingly high signal-to-noise ratio as compared to earlier work based on the stabilization of the CEP. A particular advantage of the new approach arises from the fact that the laser pulse envelope remains constant over the entire 2π phase space variation as no dispersive material needs to be used to change the CEP. The new experimental approach has been applied to study the NSDI of argon with 4 fs laser pulses at 750 nm and an intensity of 1.6×10^{14} W/cm^2. With these very short laser pulses, we observe a large (±0.5) CEP-dependent asymmetry in the recoil momentum spectra of Ar^{2+} and obtained the theoretically predicted phase-dependence of the Ar^{2+} yield. The phase-tagging approach can be utilized far beyond the studies on NSDI shown here and facilitates the detailed exploration of the waveform control of atoms, molecules, and nanoscopic objects in few-cycle laser fields.

We are grateful to Ferenc Krausz for his support and to Nikolaus Kurz from GSI Darmstadt for help in setting up the VME data acquisition system. We are further grateful for financial support from the Chemical Sciences, Geosciences, and Biosciences Division, Office of Basic Energy Sciences, Office of Science, U.S. Department of Energy, the National Science Foundation under CHE-0822646 and the DFG via PA 730/4 (GGP), the Emmy-Noether program, the International Collaboration in Chemistry program and the Cluster of Excellence: Munich Center for Advanced Photonics (MAP). GGP gratefully acknowledges support by LaserLab Europe and NGJ is grateful for support by the Fulbright commission.

References:

[1] S. Micheau *et al.*, *Phys. Rev. A* **79**, 013417 (2009).
[2] A. Baltuska *et al.*, *Nature* **421**, 611 (2003).
[3] M. F. Kling, and M. J. J. Vrakking, *Annu. Rev. Phys. Chem.* **59**, 463 (2008).
[4] E. Goulielmakis *et al.*, *Science* **320**, 1614 (2008).
[5] X. Liu *et al.*, *Phys. Rev. Lett.* **93**, 263001 (2004).
[6] G. G. Paulus *et al.*, *Nature* **414**, 182 (2001).
[7] G. G. Paulus *et al.*, *Phys. Rev. Lett.* **91**, 253004 (2003).
[8] M. F. Kling *et al.*, *Science* **312**, 246 (2006).
[9] M. F. Kling *et al.*, *Mol. Phys.* **106**, 455 (2008).
[10] M. Kremer *et al.*, *Phys. Rev. Lett.* **103**, 213003 (2009).
[11] I. Znakovskaya *et al.*, *Phys. Rev. Lett.* **103**, 103002 (2009).
[12] K. O'Keeffe *et al.*, *Appl. Phys. B* **78**, 583 (2004).
[13] T. Wittmann *et al.*, *Nature Phys.* **5**, 357 (2009).
[14] Z. Chen *et al.*, *Phys. Rev. A* **80**, 061402(R) (2009).
[15] D. N. Fittinghoff *et al.*, *Phys. Rev. Lett.* **69**, 3642 (1992).
[16] Y. Liu *et al.*, *Phys. Rev. Lett.* **104**, 173002 (2010).
[17] A. S. Alnaser *et al.*, *J. Phys. B.* **41**, 031001 (2008).
[18] O. Herrwerth *et al.*, *New J. Phys.* **10**, 025007 (2008).
[19] H. Li *et al.*, *Opt. Exp.* **16**, 20562 (2008).
[20] Q. Liao *et al.*, *J. Phys. B.* **41**, 125601 (2008).
[21] X. Liu, and C. Figueira de Morisson Faria, *Phys. Rev. Lett.* **92**, 133006 (2004).
[22] H. Rottke *et al.*, *J. Mod. Opt.* **53**, 149 (2006).
[23] A. Rudenko *et al.*, *Phys. Rev. Lett.* **93**, 253001 (2004).
[24] K. Zrost *et al.*, *J. Phys. B.* **39**, S371 (2006).
[25] M. Schultze *et al.*, *New. J. Phys.* **9**, 243 (2007).

[26] J. Ullrich *et al.*, *Rep. Prog. Phys.* **66**, 1463 (2003).
[27] F. Lindner *et al.*, *Phys. Rev. Lett.* **92**, 113001 (2004).
[28] G. G. Paulus *et al.*, Patent No. 102010019814.5 (2010).
[29] A. M. Sayler *et al.*, *Opt. Lett.*, in press (2010).
[30] A. J. Verhoef *et al.*, *Opt. Lett.* **31**, 3520 (2006).
[31] J. Rauschenberger *et al.*, *Las. Phys. Lett.* **3**, 37 (2006).

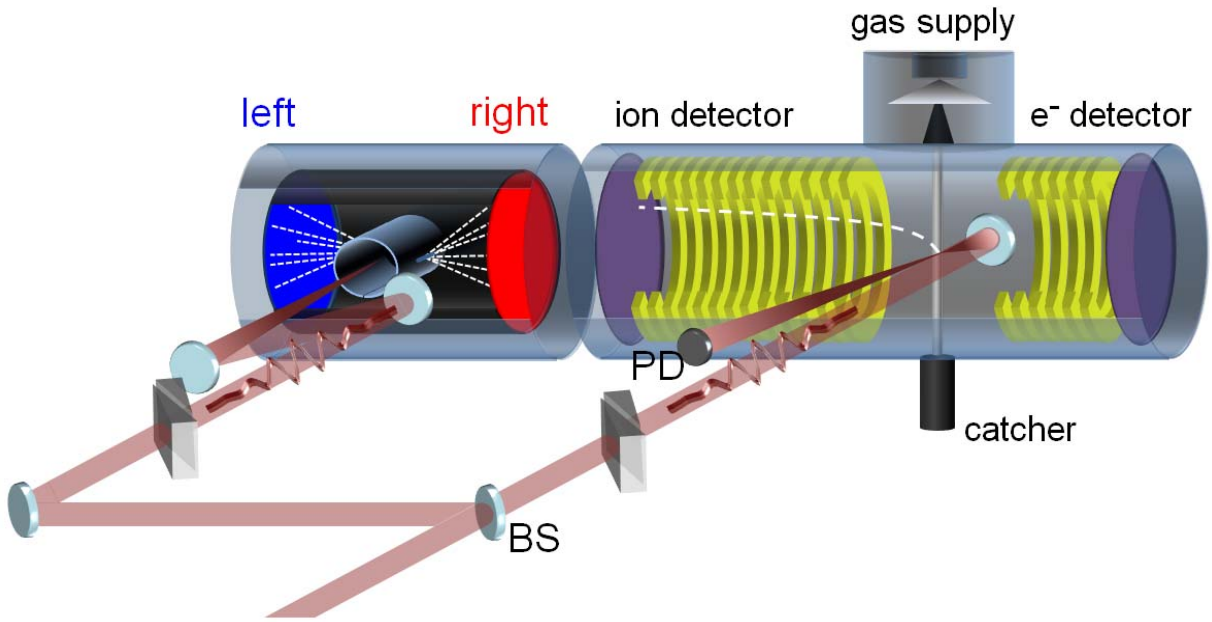

FIG. 1 (Color online) Schematic of the setup consisting of a single-shot stereo-ATI phase meter (left chamber) and a REMI spectrometer (right chamber). A beamsplitter (BS) directs light into both chambers. Each arm is equipped with its own wedges for compensating residual chirp. The phase meter contains a layer of μ-metal to shield from external electric and magnetic fields. A Xe gas pressure of 6.5×10^{-3} mbar fills the inner gas cell. In the Stereo-ATI, xenon atoms are ionized near the focus of the horizontally polarized laser beam and the electrons produced enter the high-vacuum drift tubes through slits. Electrons resulting from the ionization by a single laser shot are detected by MCP detectors to the left and to the right, enabling the determination of the CEP for each REMI event as described in the text. Simultaneously, Ar^{2+} ions created in the overlap of the laser focus and a skimmed supersonic jet of the REMI are detected by an MCP and delay line detector. The jet stream is efficiently pumped by the catcher. The master trigger for the electronics is provided by a fast photodiode (PD). Note that the ion and electron optics are symmetric in reality and a few electrodes have been removed for visualization of the laser path. Furthermore, the electron detection, which is facilitated by additional magnetic fields, was not utilized in these first proof-of-principle experiments, where only ions were detected.

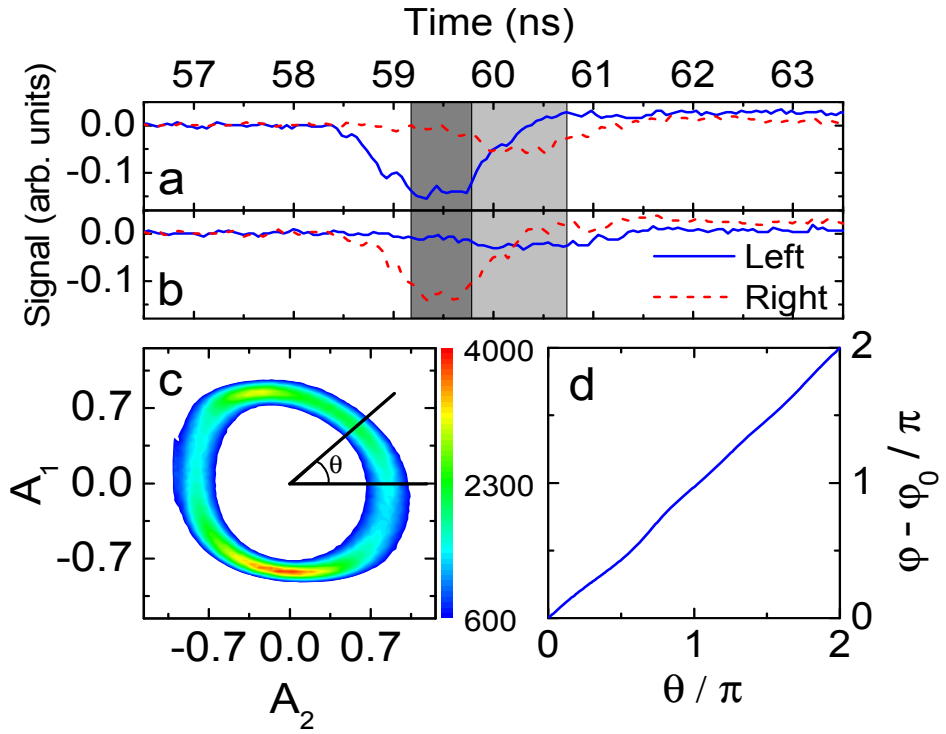

FIG. 2. (Color online) a) and b) Time-of-flight traces from the left and right detectors of the Stereo-ATI for two laser shots with different CEPs. Light and dark shaded areas indicate the gated regions for determining A_1 and A_2, respectively. c) Parametric asymmetry plot (PAP) taken under the same conditions as the Ar^{2+} data (see text for further details). The color scale indicates the number of counts. d) The relative CEP, φ-φ_0, as a function of the polar angle in the PAP, θ. The small deviation from the line φ-$\varphi_0 = \theta$ indicates only minor adjustments are needed for retrieving the correct relative phase.

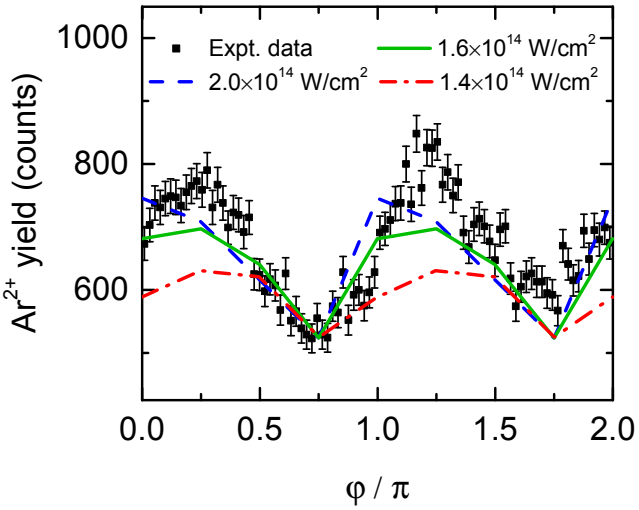

FIG. 3. (Color online) Comparison of the experimental CEP-dependent Ar^{2+} yield (filled black squares) with theoretical predictions (colored lines) for three different intensities from Micheau *et al.* [1]. The error bars indicate the statistical error of the experimental data. The offset phase, $\varphi_0 = 0.43\pi$, for the experimental data has been chosen, such that the minimum in the experimental data coincides with the theory.

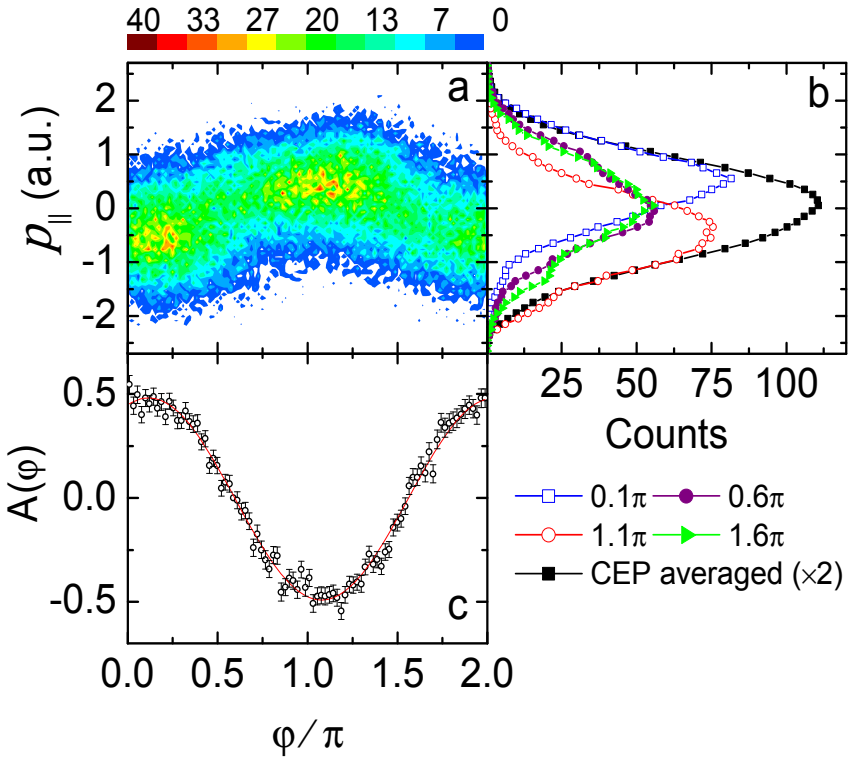

FIG. 4. (Color online) Experimental results for NSDI of argon showing a) the CEP dependence of the Ar^{2+} longitudinal momentum along the laser polarization axis ($p_{||}$), b) longitudinal Ar^{2+} momentum spectra for the CEP averaged (filled black squares) and four phases φ as indicated in the legend (integrated within $\pm 0.04\pi$ and averaged over 5 adjacent $p_{||}$ values), c) the asymmetry parameter, $A(\varphi)$ as defined in the text. The error bars denote the statistical error.